Joint Pathology Center

Veterinary Pathology Services

WEDNESDAY SLIDE CONFERENCE 2016-2017

C o n f e r e n c e 17

1 February 2017

CASE I: 12A208 (JPC 4017925).

Signalment: Three-year-old, male, pigtail macaque, (*Macaca nemestrina*).

History: This animal was inoculated intravenously with SIVmac239, 177 days prior to humane sacrifice. It had a history of intermittent diarrhea, weight loss, mild dehydration, and upper respiratory signs (sneezing and nasal discharge). The day before sacrifice the animal began vocalizing and became progressively ataxic.

Gross Pathology: The animal was thin with atrophic thymus and peripheral nodes but enlarged mesenteric and internal iliac nodes. Distal esophageal mucosa was covered with a proliferative growth of *Candida sp*. The colon had a thickened mucosa and was dilated with fluid feces.

Laboratory results: *Moraxella sp*. and hemolytic staphylococcus were cultured from the nasal cavity. *Balantidium coli* and *Trichuris trichiura* were identified by fecal flotation. Cytomegalovirus was identified by PCR in paraffin sections of testis.

Histopathologic Description: The section of testis includes edematous rete testis with canaliculi, lobules made up of immature seminiferous tubules with multiple zones of necrosis, and thickened, inflamed, and partially fused tunica albuginea and vaginalis. Complete and partial lobules are destroyed by multifocal to coalescing coagulative necrosis involving seminiferous tubules and interstitium. Segments of small and medium-sized vessels are necrotic with hyalinized walls, fibrin thrombi and infiltration of neutrophils. Sertoli cells within the tubules, numerous Leydig cells, fibrocytes and myoid cells adjacent to the basal lamina of the tubules, and fibroblasts and endothelium lining interstitial vessels contain large round, oval, tear-drop and occasionally lobulated and multiple eosinophilic intranuclear inclusions usually surrounded by a clear halo. Some enlarged cells have additional amorphous granular eosinophilic aggregates within the cytoplasm. Interstitial stroma of the mediastinum, lobules, and both tunics is severely edematous with fibrin deposition, microhemorrhages, microthrombi, and predominantly neutrophilic infiltration, especially around small vessels. Neutrophils

are necrotic, fragmented and mixed with small numbers of eosinophils.

Contributor's Morphologic Diagnosis: Acute orchitis with multifocal to coalescing, coagulative and fibrinoid necrosis, intravascular fibrin thrombi and intranuclear inclusions, Cytomegalovirus, Testis

Contributor's Comment: Cytomegalovirus (CMV) is a betaherpesvirus comparable in sequence and pathogenesis to species-specific CMV of monkeys, humans, and other animals. CMV of Rhesus and Japanese macaques, African green monkeys (AGM), and chimps have distinct restriction fragment profiles.[1,6] Uncomplicated infections rarely cause disease, even in infants, usually become latent, and may reactivate later in life due to the immunosuppression of viral infection, cancer treatment, or organ transplantation. In breeding colonies, 50% of infants become seropositive by six months and nearly 100% by one year.[3] Transmission via breast milk,

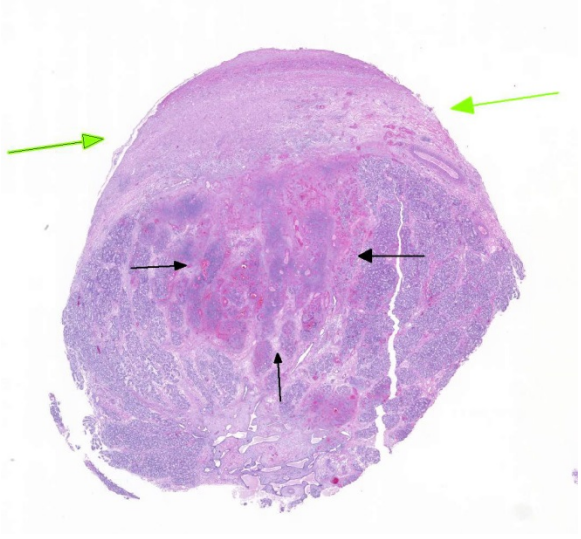

Testis, cynomolgus macaque. At low magnification, there is a large infarct at the edge of the testis (black arrows). The overlying tunics are fused. (HE, 5X)

saliva, and possibly urine[2] seem likely routes of transmission; transplacental infection is possible but rare[2]; transplantation of infected organs is a documented risk.[12]

The incidence of CMV disease in monkeys with SAIDS is variable but can be as high as 30-50% of seropositive animals.[12,15] Tissues displaying cytomegalic cells containing intranuclear inclusions include central and peripheral nervous system, lung, lymph nodes, liver, GI tract, testis, and arteries[4].

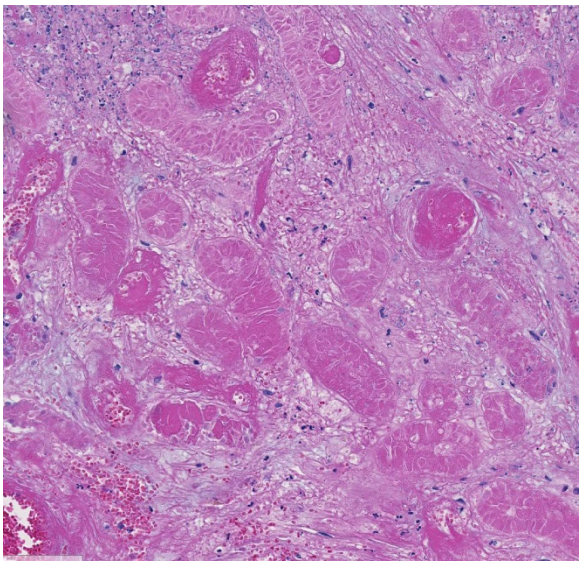

Testis, cynomolgus macaque. Higher magnification of the area of testicular infarction. (HE, 128X)

CMV disease in SIV-infected monkeys can be predicted by prolonged detection of CMV DNA in plasma and a decrease in anti-CMV titer and avidity[14]. Profound depletion of CD8 T cells (once thought linked[9]) is less important than the expanded target cell pool of activated CD4 cells.[4]

Genomes for rhesus and chimp CMV are sequenced and partial sequences for AGM and baboon CMV are reported.[6,7] There is a strong conservation of coding content between human and simian CMV, with even closer homologies among CMV of closely related primate hosts. While estimates of open reading frames in rhesus CMV vary

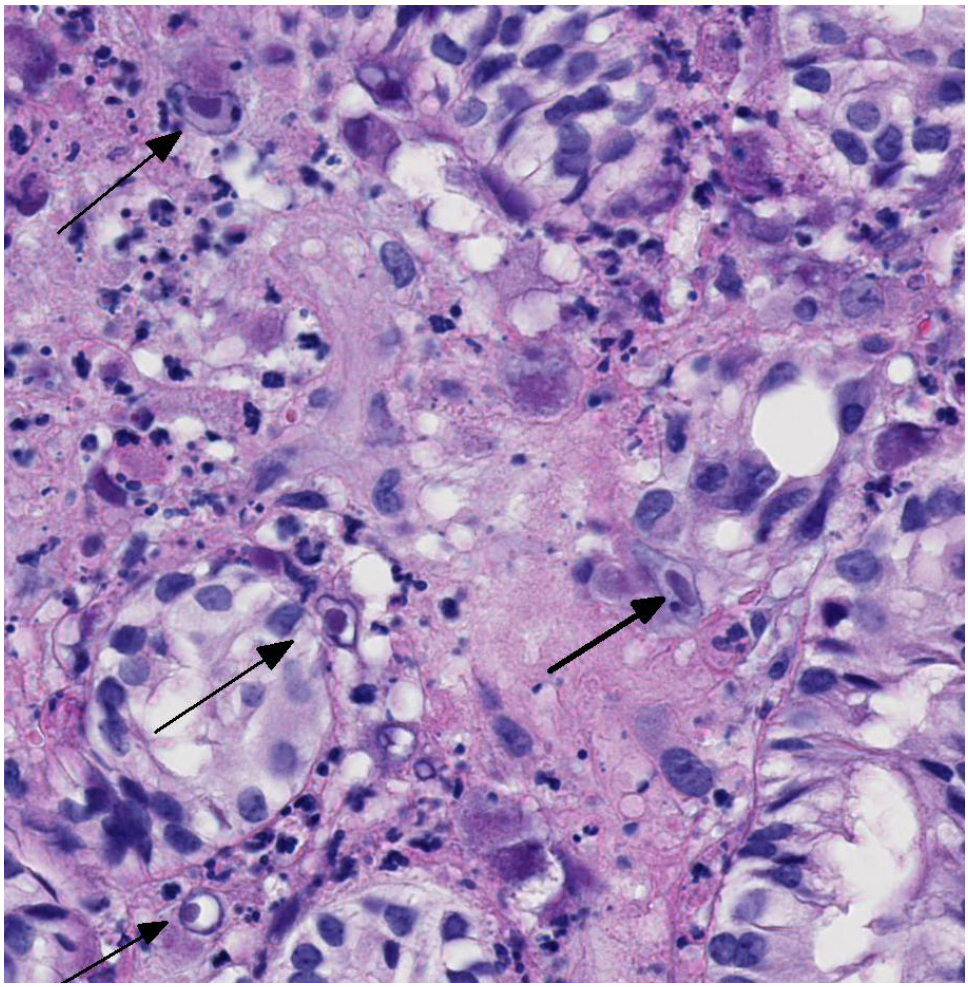

Testis, cynomolgus macaque. Necrotic seminiferous tubules often contain cytomegalic cells with a prominent karyomegalic inclusion (black arrows) characteristic of cytomegalovirus. (HE, 400X)

from 230-258 genes, it is clear that evolution has produced extra coding capacity in rhesus compared to human and chimp CMV.[3] Sequence homology demonstrates codes for proteins critical for neutrophil activation by CXC chemokines, TNF receptor, B-chemokine receptor, and IL-10 in rhesus CMV. In human fibroblasts, CMV can change levels of more than 250 cellular genes including cyclooxygenase 2 (COX-2)[17], which converts arachidonic acid (AA) to prostaglandin endoperoxide H. Rhesus CMV does not increase cellular COX-2 but produces a homologue protein[6] that could be used to modulate the host inflammatory process.

CMV establishes life-long infection in immunocompetent hosts in sites of latency and persistent infection. During latency, infected cells demonstrate limited viral gene expression, while in persistently infected cells; virions are continuously produced with minimal cytopathic effect. Endothelial cells, myeloid cells (particularly CD14+ monocytes) and possibly smooth muscle cells in large arteries are the likely sites of infection and latency.[9] CMV infection of endothelial cells increases expression of cell adhesion molecules (ICAM-1) which interacts with monocytes and could provide a means for distribution. Infected cells induce a vigorous immune response releasing pro-inflammatory cytokines (like gamma IFN and TNF-alpha) that play a role in reactivation[15]. Monocyte differentiation driven by con-A-stimulated T-cells has been shown to reactivate non-lytic infection in monocyte-derived macrophages as well as other myeloid precursors[7]. The precise combination of cells and mediators may vary depending on the system but inflammatory cytokines, chemokines, and even some anti-inflammatory cytokines like

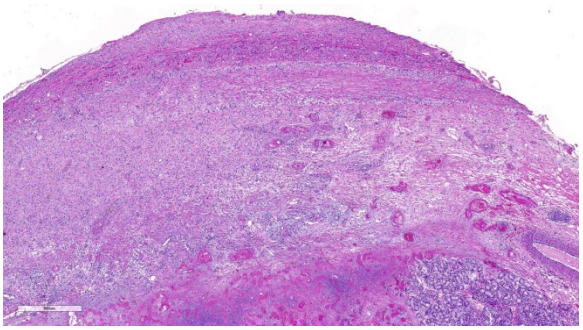

Testis, cynomolgus macaque. The overlying tunics are fused and expanded by abundant fibrous connective tissue. (HE, 20X)

IL-10 play a role in reactivation. The ability of CMV to bind to Fc-domains of neutralizing antibody and use it to infect naïve cells[13] enhances viral persistence. In one study all SIV-infected rhesus monkeys were latently infected with CMV, seven of eleven had productive infections demonstrated by immunohistochemistry in the gut, liver, lungs, and testicles, and two of these seven had typical inflammatory lesions.[11]

Our case demonstrates reactivation of CMV in the testis. Large numbers of classic "owls-eye" cells are noted in the endothelium and interstitial cells extending Baskin's earlier observations.[5] Evidence of vascular thrombosis could have contributed to the extensive necrosis observed in this tissue.

JPC Diagnosis: Testis: Coagulative necrosis (infarct), focally extensive, with vascular thrombosis, fibrinoid necrosis, chronic periorchitis with adhesions, and intranuclear viral inclusions, pigtail macaque, *Macaca nemestrina*.

Conference Comment: Rhesus cytomegalovirus (CMV), also known as macacine herpesvirus-3, is the most common opportunistic pathogen in SIV-infected rhesus macaques with a seroprevalence approaching 100% within the first year of life. Other nonhuman primates with host-adapted CMVs include chimpanzees, African green monkeys, sooty mangabeys, and owl monkeys.[2,3,4,6] These highly host-specific dsDNA viruses of the subfamily betaherpesvirinae have tropism for multiple organs producing interstitial pneumonia, gastroenteritis, poly-radiculoneuritis, encephalitis, and lymphadenitis, in addition to orchitis and periorchitis present in this case.[2] Lesions may also be in the liver, spleen, salivary gland, lymph node, and kidney. Both human and rhesus CMV are unique in that they encode a CXC chemokine, interleukin 8 (IL-8), which induces neutrophil chemotaxis, a prominent feature in this case.[2] This tissue section has marked karyomegaly and cytomegaly with prominent magenta intranuclear inclusions, typical for CMV. Necrotizing and proliferative vasculitis has also been reported in affected tissues.[2,3] In this case, there is fibrinoid vascular necrosis with thrombosis, which likely caused a focally extensive area of coagulative necrosis (infarct) in this testis.

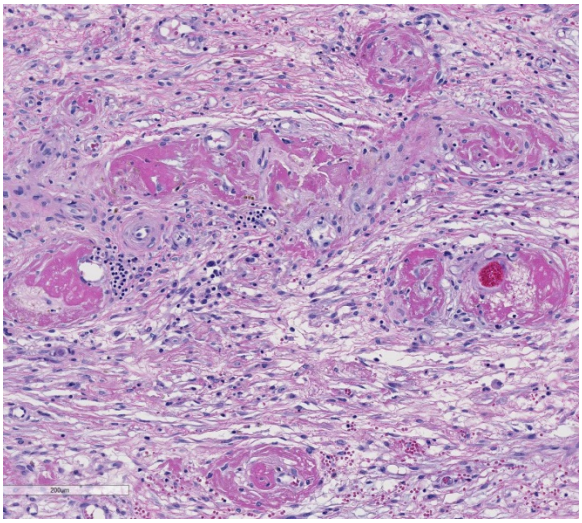

Testis, cynomolgus macaque. Blood vessels with in the fused tunics exhibit fibrinoid necrosis. (HE, 128X)

Additionally, a recent report in *Veterinary Pathology*[2] reported peripheral neuropathy in the facial nerve associated with systemic CMV infection in a group of SIV-positive rhesus macaques. Interestingly, the pathogenesis of the nerve damage is likely due to the bystander effect secondary to CMV-induced inflammation rather than direct viral infection of Schwann cells.[2] Readers are encouraged to review 2015 Wednesday Slide Conference 16 Case 1 for a great example of CMV-induced radiculitis within lumbar spinal roots of a rhesus macaque.

Conference participants discussed other cytomegaloviruses of veterinary importance. Guinea pig cytomegalovirus, also known as Cavid herpesvirus 1, is a common incidental finding in immunocompetent guinea pigs. Similar to CMV of other species, the salivary glands are the primary target tissue in the guinea pig.[15] Additionally, suid herpesvirus 2 is a CMV that affects pigs causing inclusion body rhinitis in suckling pigs and severe generalized disease in neonates (>3 weeks old).[18] Hamster, mice, and rats also have their own host adapted CMVs typically affecting the salivary and lacrimal glands.[15]

Contributing Institution:
Tulane National Primate Research Center
Department of Comparative Pathology
18703 Three Rivers Rd
Covington, LA 70433
http://www.tnprc.tulane.edu/

References:

1. Alcendor DJ, Barry PA, Pratt-Lowe E, Luciw PA. Analysis of the rhesus cytomegalovirus intermediate-early gene promoter. *Virology*. 1993;194:815-821.
2. Assaf BT, Knight HL, Miller AD. Rhesus cytomegalovirus (*Macacine herpesvirus-3*) associated facial neuritis in a simian immunodeficiency virus infected rhesus macaques. *Vet Pathol.* 2015; 52(1):217-223.
3. Barry PA and Chang WL. Primate betaherpesviruses. In: *Human Herpesviruses: Biology, Therapy, and Immunoprophylaxis*. Cambridge: Cambridge University Press; 2007.
4. Barry AP, Silvestri G, Safrit JT et al. Depletion of CD8+ cells in sooty mangabey monkeys naturally infected with simian immuno-deficiency virus reveals limited role for immune control of virus replicated in a natural host species. *J Immunol*. 2007; 178(12):8002-8012.
5. Baskin GB. Disseminated cyto-megalovirus infection in immuno-deficient rhesus monkeys. *Am J Path*. 1987; 29(2):345-352.
6. Davison AJ, Dolan A, Akter P et al. The human cytomegalovirus genome revisited: comparison with the chimpanzee cytomegalovirus genome. *J Gen Virol*. 2003; 84(1):17-28.
7. Hansen SG, Strelow LI, Franchi DC et al. complete sequence and genomic analysis of rhesus cytomegalovirus. *J Virol*. 2003; 77:6620-6636.
8. Ibanez CE, Schrier R, Ghazal P et al. A human cytomegalovirus productively infects primary differentiated macrophages. *J Virol*. 1991; 65:6581-6588.
9. Jarvis MA, Nelson JA. Molecular basis of persistence and latency. In: *Human Herpesvirus Biology, Therapy, and Immunoprophylaxis*. Cambridge University Press, 2007.
10. Kaur A, Daniel MD, Hempel D et al. Cytotoxic T-lymphocyte responses to cytomegalovirus in normal and

simian immunodeficiency virus-infected rhesus macaques. *J Virol*. 1996; 70(11):7725-7733.
11. Kuhn EM, Stolte N, Matz-Rensing K et al. Immunohistochemical studies of productive rhesus cyto-megalovirus infection in rhesus monkeys (*Macaca mulatta*) infected with simian immunodeficiency virus. *Vet Pathol*. 1999; 36(1):51-56.
12. Lee So, Razonable RR. Current concepts on cytomegalovirus infection after liver transplantation. *World J Hepatol*. 2010; 2(9):325-326.
13. Manley K, Anderson J, Yang F, et al. Human cytomegalovirus escapes a naturally occurring neutralizing antibody by incorporating it into assembling virions. *Cell Host Microbe*. 2011; 10:197-209.
14. Osborn KG, Prahalada S, Lowenstine LJ et al.The pathology of an epizootic of acquired immuno-deficiency in rhesus macaques. *Am J Pathol*. 1984; 114:94-103.
15. Percy DH, Barthold SW. *Pathology of Laboratory Rodents and Rabbits*, 4th ed. Ames, IA: Blackwell Publishing; 2016:15,122,175,219.
16. Sequar G, Britt WJ, Lakeman FD et al. Experimental coinfection of rhesus macaques with rhesus cytomegalovirus and simian immunodeficiency virus: Pathogenesis. *J Virol*. 2002; 76(15):7661-7671.
17. Waldman WJ, Knight DA, Cytokine-mediated induction of endothelial adhesion molecule and histo-compatibility leukocyte antigen expression by cytomegalovirus-activated T cells. *J Inf Dis*. 1995; 171:263-272.
18. Yoon KJ, Edington N. Porcine cytomegalovirus. In: Straw BE, et al, eds. *Diseases of Swine*. 9th ed. Ames, IA:Blackwell Publishing; 2006:323-329.
19. Zhu H, Cong JP, Mamtora G et al. Cellular gene expression altered by human cytomegalovirus: global monitoring with oligonucleotide arrays. *Proc Natl Acad Sci* 1998; 95(24):14470-14475.

CASE II: T1339/16 (JPC 4085507).

Signalment: Unknown age and gender, guinea pig, (*Cavia porcellus*).

History: The animal developed a skin tumor of 1 cm in diameter at the right flank. The mass was completely resected. Unfortunately, further clinical data were not available.

Gross Pathology: A 2 x 1 cm skin sample was submitted for histopathologic examination. Centrally there was a well-demarcated, 1 x 1 cm partially exophytic firm nodule. The cut surface was light brown.

Laboratory results: Immuno-histochemically the neoplastic cells were positive for Melan-A and PNL2.

Histopathologic Description: Haired skin: Elevating an ulcerated epidermis and infiltrating into the underlying dermis (in some slides, tumor overlies an intact epidermis) is densely cellular, well-demarcated, exophytic, partly infiltrative and ulcerated, unencapsulated neoplasm composed of sheets of pleomorphic round cells within a scant fibrovascular stroma. Neoplastic cells are round to polygonal, up to 40 um in diameter with variable distinct cell borders and moderate amounts of

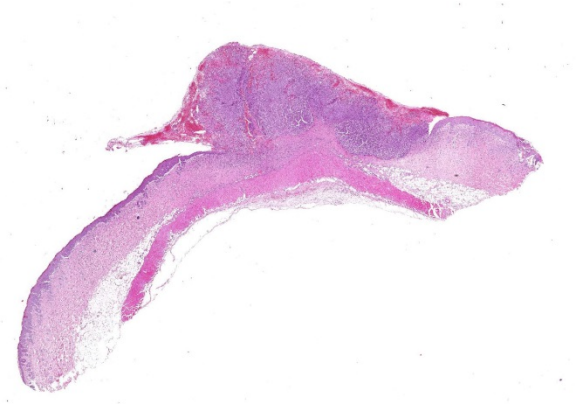

Haired skin, rabbit. Infiltrating the dermis, there is a 1cm, moderately cellular, exophytic neoplasm. (HE, 5X).

eosinophilic cytoplasm. Nuclei are round to oval, centrally located with finely stippled chromatin and up to four prominent magenta nucleoli. Mitoses average 2-3 per high power field (some bizarre) and cells show moderate anisocytosis and anisokaryosis. Occasionally, vascular invasion of tumor cells can be observed (not in all slides). There are multifocal hemorrhages within and around the tumor and hemorrhagic and serocellular crusts at the ulcerated surface. The adjacent skin is hyperplastic with a moderate perivascular infiltration with lymphocytes, plasma cells, and few heterophils.

Contributor's Morphologic Diagnosis: Haired skin: Amelanotic malignant melanoma, guinea pig, *Cavia porcellus*

Contributor's Comment: Melanomas are described in a variety of animal species including domestic animals and wildlife species. However, they are most common in dogs, horses and some breed of swine[10], only few reports of melanoma in birds, laboratory animals and more recently in reptiles exist.[6,16] The histologic diagnosis of melanoma is complicated due to variable degree of pigmentation and the high variability of cell shapes. With the help of immunohistochemistry, most amelanotic melanoma can be routinely diagnosed.[3,4,10]

With our case, we present a well-known neoplasm in an unusual species. Case reports of spontaneous melanoma in the guinea pig are extremely rare, but the guinea pig is a well-defined model of experimental melanoma using the potent carcinogen 7,12-dimethylbenz[*a*]anthracene (DMBA), a polycyclic aromatic hydrocarbon.[7] This substance is proven to transform cells in different oncogenic pathways.[2]

Mutations that affect cell cycle control (p16/INK4a, CDK4), pro-growth pathways (growth factor receptors, RAS, BRAF), and telomerase were identified in the patho-genesis of malignant melanoma. Furthermore, melanomas can be inherited, and UV light-induced DNA damage plays a role as do other factors.[8]

The most common naturally occurring skin tumors in guinea pigs are trichofolliculomas. They are a subtype of trichoepithelioma and occur as expansible, often centrally cystic neoplasia in the skin often of the lumbosacral region.[13,15,18] Other tumors, like fibrosarcoma, lipoma, sebaceous gland adenoma, and hemangioma were also reported in this species.

In this melanoma, there is abundant vascularity. As observed in other species[5,12] the amount of blood vessels may be a prognostic factor for this neoplasia in guinea pigs, and particularly mast cells may play a significant role in angiogenesis as the major source of VEGF.[1]

Unfortunately, further information regarding the clinical course of the presented case was not available.

JPC Diagnosis: Haired skin: Amelanotic melanoma, guinea pig, *Cavia porcellus*.

Conference Comment: Melanocytic neoplasms arise from melanocytes or melanoblasts which are derived from the neural crest ectoderm. As mentioned by the contributor, melanomas have been identified in most veterinary species and humans. The histologic diagnosis of melanomas is sometimes complicated due to the variability of pigmentation and arrangement of neoplastic cells into clear cells (balloon cell), spindle cell, epithelioid cell, and signet ring cell histomorphology.[10] Additionally, there are often multiple different tumor cell morphologies within a single neoplasm. For this reason, melanomas are sometimes referred to as one of the "great imitators" due to their common embryologic connection with both neural and epithelial origin.[10] This case nicely demonstrates this point, due to variation in round to polygonal cellular appearance across various regions of the neoplasm. Despite the rarity of melanocytic neoplasms in guinea pigs and the lack of melanin granularity in this case, most conference participants included amelanotic melanoma high within their differential diagnosis. Prior to the conference, the Joint Pathology Center ran the histochemical stain Fontana-Masson and immuno-histochemical stains melan-A and S100. The Fontana-Masson stain highlighted multifocal positive argentaffin granules and melanin within the cytoplasm of neoplastic cells. Additionally, neoplastic cells are immunopositive for S100 and melan-A red, confirming the diagnosis of an amelanotic melanoma, in this case.

As mentioned by the contributor, trichofolliculomas are the most common tumor in the skin of guinea pigs; although, spontaneous neoplasms in this species are rare in animals under three years old.[13]

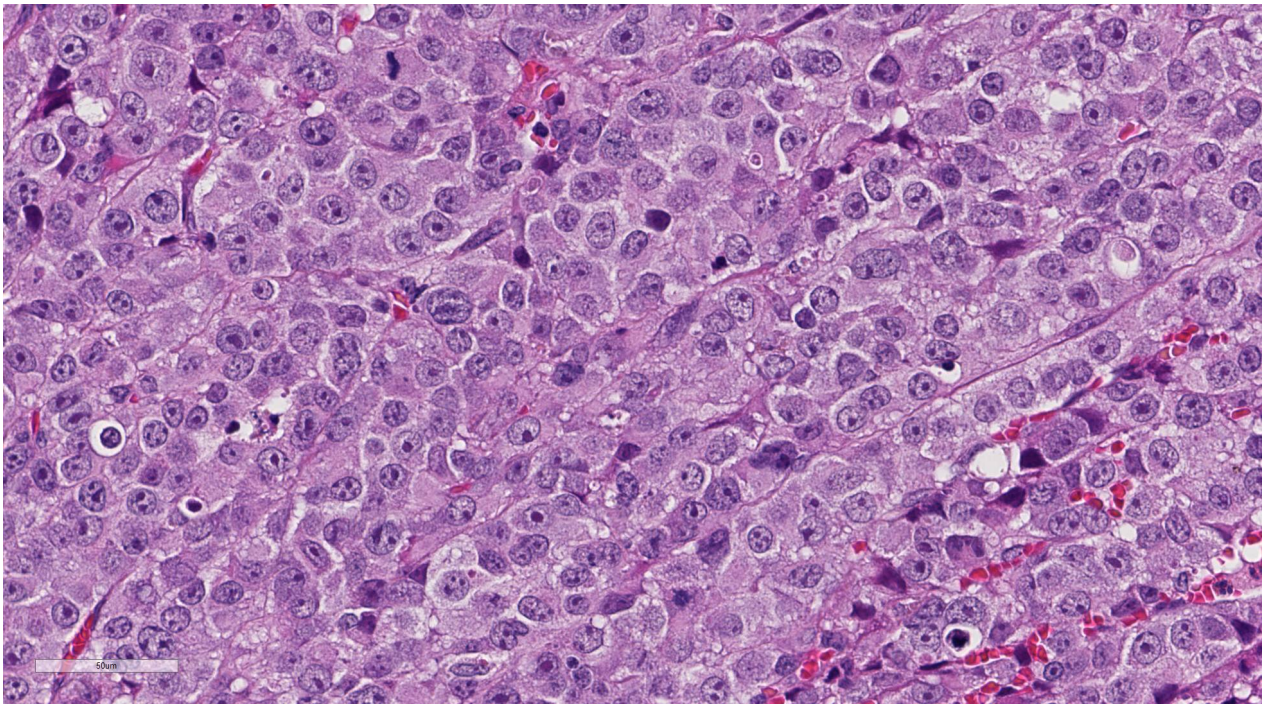

Haired skin, rabbit. Neoplastic cells are polygonal, arranged in nests and cords with abundant granular cytoplasm, and have large nuclei with prominent nucleoli. Mitotic figures are common.

These benign dome-shaped subcutaneous nodules, typically less than 2cm in diameter, most commonly occur along the dorsal lumbar region and may represent a hamartomatous rather than a neoplastic process.[10,13] Trichofolliculoma development is thought to occur secondary to inhibition of bone morphogenic protein (BMP), an important tumor suppressor gene.[13,14,18] Studies indicate that BMP plays a critical role in maintaining homeostasis of hair follicles and regulation of skin development.[14] In addition, BMP is an important growth factor for a variety of tissues throughout the body and its con-centration is tightly regulated in health. Interestingly, recent research in humans have shown that absence of BMP signaling leads to the progression of colorectal carcinoma; conversely, overexpression of BMP signaling induces epithelial-mesenchymal transition, tumor invasion, and metastasis in a variety of malignant neoplasms.[9,11,14]

Contributing Institution:
Institut fuer Veterinaer-Pathologie, Justus-Liebig-Universitaet Giessen
Frankfurter Str. 96, 35392
Giessen, Germany
http://www.uni-giessen.de/cms/fbz/fb10/institute_klinikum/institute/pathologie

References:

1. Ch'ng S, Wallis RA, Yuan L, Davis PF, Tan ST. Mast cells and cutaneous malignancies. *Mod Pathol*. 2006; 19(1):149-159.
2. Currier N, Solomon SE, Demicco EG, Chang DL, Farago M, Ying H, Dominguez I, Sonenshein GE, Cardiff RD, Xiao ZX, Sherr DH, Seldin DC. Oncogenic signaling pathways activated in DMBA-induced mouse mammary tumors. *Toxicol Pathol.* 2005;33(6):726-37.
3. Goldschmidt MH, Dunstan RW, Stannard AA, Tscharner CV, et al. *Histological classification of epithelial and melanocytic tumors of the skin of domestic animals*. Vol III. 2nd series. Washington D.C.: Armed Forces Institute of Pathology. 1998.
4. Goldschmidt MH, Hendrick MJ. Tumors of the skin and soft tissue. In: Meuten DJ, ed. *Tumors in Domestic Animals*. 4th Ed. Ames, IA, USA: Blackwell Publishing; 2002:45-117.
5. Gregório H, Raposo TP, Queiroga FL, Prada J, Pires I. Investigating associations of cyclooxygenase-2 expression with angiogenesis, proliferation, macrophage and T-lymphocyte infiltration in canine melanocytic tumours. *Melanoma Res*. 2016; 26(4):338-347.
6. Heckers KO, Schmidt V, Krastel D, Hildebrandt G, Kiefer I, Pees M. Malignant melanophoroma in a Hermann's tortoise (*Testudo hermanni*). A case report. *Tierarztl Prax* (K) 2011; 39:45-50.
7. Ingram AJ. Review of chemical and UV light-induced melanomas in experimental animals in relation to human melanoma incidence. *J Appl Toxicol*. 1992; 12(1):39-43.
8. Lazar AJF, Murphy GF. The skin. In: Kumar Abbas Aster Robbins and Cotran. *Pathologic basis of disease*. 9th Edition. Philadelphia, PA, Elsevier Saunders. 2015. 1147-1150.
9. Kan L, Liu Y, et al. Inhibition of BMP signaling in P-cadherin positive hair progenitor cells leads to tricho-folliculoma-like hair follicle neoplasms. *J Biomed Sci*. 2011; 14:92.
10. Mauldin EA, Peters-Kennedy J. Integumentary system. In: Maxie MG, ed. *Jubb, Kennedy and Palmers Pathology of Domestic Animals*. 6th ed.

Vol 1. Elsevier, St. Louis, Missouri; 2016:705,720-736.
11. Owens p, Pickup MW, et al. Inhibition of BMP signaling suppresses metastasis in mammary cancer. *Oncogene*. 2015; 34:2437-2449.
12. Pastushenko I, Vermeulen PB, Carapeto FJ, Van den Eynden G, Rutten A, Ara M, Dirix LY, Van Laere S. Blood microvessel density, lymphatic microvessel density and lymphatic invasion in predicting melanoma metastases: systematic review and meta-analysis. *Br J Dermatol*. 2014; 170(1):66-77.
13. Percy DH, Barthold SW. *Pathology of Laboratory Rodents and Rabbits*, 4th ed. Ames, IA: Blackwell Publishing; 2016:251.
14. Sharov AA, Mardaryev AN, Sharova TY, Grachtchouk M, Atoyan R, Byers HR, Seykora JT, Overbeek P, Dlugosz A, Botchkare VA. Bone morphogenetic protein antagonist noggin promotes skin tumorigenesis via stimulation of the Wnt and Shh signaling pathways. *Am J Path*. 2009; 175(3):1303-1314.
15. Sommerey CC, Köhler K, Reinacher M. Erkrankungen des Meerschweinchens aus Sicht der Pathologie. *Tierarztl Prax* (K) 2004; 32:377-383.
16. Thompson KA, Campbell M, Levens G, Agnew D. Bilaterally symmetrical oral amelanotic melanoma in a Boa constrictor (Boa constrictor constrictor). *J Zoo Wildl Med*. 2015; 46(3):629-32.
17. Voorneveld PW, Kodach LL, et al. Loss of SMAD4 alters BMP signaling to promote colorectal cancer cell metastasis via activation of Rho and ROCK. *Gastroenterology*. 2014; 147:196-208.
18. Williams BH. Non-infectious disease. III Guinea pigs. In: Suckow MA, Stevens KA, Wilson RP. *The laboratory rabbit, guinea pig, hamster and other rodents*. First Edition. London, Waltham, MA, San Diego, CA. Elsevier, Academic press, 2012, 685-704.

CASE III: 11A228 (JPC 4019364).

Signalment: Nine-year-old, female, rhesus macaque, (*Macaca mulatta*).

History: This adult female rhesus macaque was imported from China by a commercial vendor and completed international quarantine. It was acquired by this institution in December 2009 and completed domestic quarantine in January 2010. Multiple tests for tuberculosis were performed. The animal was housed individually in a room with 11 other adult rhesus macaques. Euthanasia and necropsy were performed when other animals housed in this room exhibited positive reactions to intradermal skin tests using mammalian old tuberculin (MOT).

Gross Pathology: A single 0.3cm firm nodule containing homogenous off-white

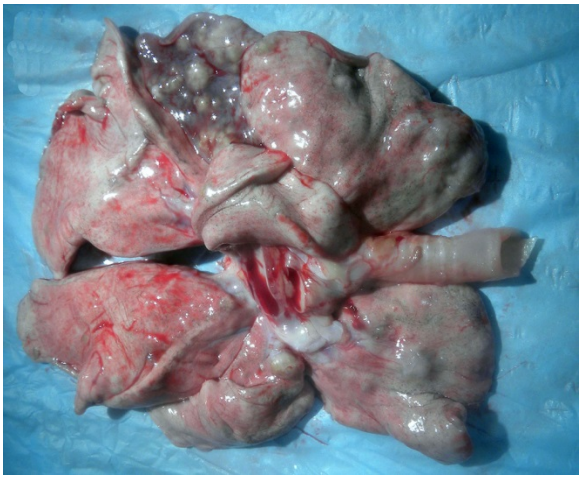

Tracheobronchial lymph nodes, rhesus macaque. These nodes are largely effaced by granulomas which bulge from the cut surface. (Photo courtesy of: Oregon National Primate Research Center, http://onprc.ohsu.edu).

material was present within the parenchyma of the right caudal lung lobe. There were several pale gray foci within the lung lobes measuring approximately 0.3 cm in diameter. All lung lobes exhibited diffuse, fine, gray-black stippling, consistent with anthracosilicosis. The tracheobronchial lymph nodes were moderately enlarged and distorted by multiple nodules. On sectioned surface the nodules contained cores of off-white material with a firm tan rim. The remaining lymph node parenchyma was dark gray.

Laboratory results:

Table 1: Eyelid scoring guide, intradermal tuberculin skin test (TST) with MOT:

Grade	Score	Description
0	Negative	No reaction
1	Negative	Bruise
2	Negative	Erythema, no swelling
3	Suspect	Erythema with minimal swelling OR slight swelling without erythema
4	Positive	Obvious swelling with eyelid droop and erythema
5	Positive	Swelling and/or necrosis with eyelid closed

Table 2: Tuberculosis testing

Date	Test	Result
12-14-09	TST MOT	Grade 0 (negative)
12-28-09	TST MOT	Grade 0 (negative)
01-05-10	Thoracic radiographs	unremarkable
01-11-10	TST MOT	Grade 0 (negative)
11-05-10	TST MOT	Grade 3 (suspect)
11-08-10	TST MOT	Grade 0 (negative)
11-08-10	PRIMAGAM®	Negative
11-08-10	PrimaTB STAT-PAK®	Negative
04-08-11	PrimaTB STAT-PAK®	Negative
04-14-11	PrimaTB STAT-PAK®	Negative

Histopathologic Description: The normal architecture of the lymph node is multifocally effaced and expanded by round to irregular granulomas (tubercles) characterized by variable central accumulations of homogeneous eosinophilic material and cellular and karyorrhectic debris admixed with neutrophils and surrounded by an inner rim of foamy, epithelioid macrophages, occasional multi-nucleated giant cells (Langhans type), fibroblasts, bands of eosinophilic material (collagen), and an outer rim of lymphocytes and fewer histiocytes. Numerous histiocytes in the medullary sinuses contain cytoplasmic granules that are black to brown and occasionally refractile (anthracosilicotic pigment). A Ziehl-Neelsen stain reveals rare acid-fast bacilli in epithelioid macrophages and multinucleated giant cells.

Contributor's Morphologic Diagnosis: Tracheobronchial lymph node: Lymphadenitis, necrogranulomatous, chronic, multifocal, moderate, with rare intracellular acid-fast bacilli, rhesus

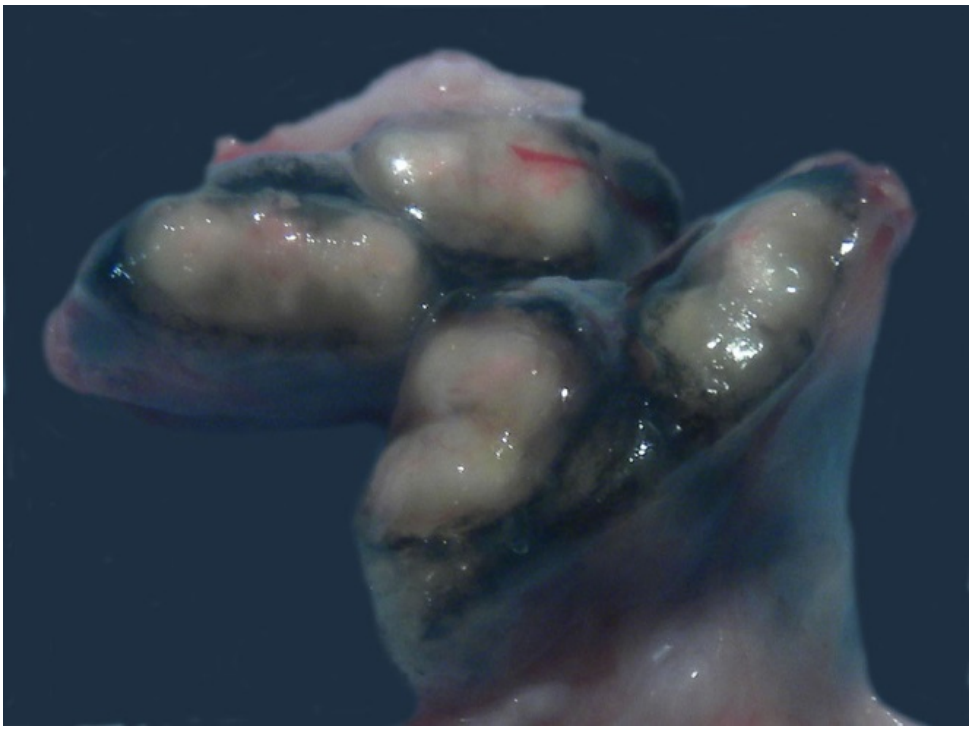

Lungs, rhesus macaque. Variably-sized granulomas are present within multiple lung lobes. (Photo courtesy of: Oregon National Primate Research Center, http://onprc.ohsu.edu).

macaque (*Macaca mulatta*), nonhuman primate.

Relevant microscopic findings of tissues not submitted: Similar focus of necro-granulomatous inflammation containing rare intracellular acid-fast bacilli in epithelioid macrophages and multi-nucleated giant cells was present in the lung.

Contributor's Comment: This was a case of spontaneous tuberculosis affecting a single room housing 12 rhesus macaques (*Macaca mulatta*). The primary gross and histologic findings are necrogranulomatous inflammation with rare intracellular acid-fast bacilli involving multiple tracheobronchial lymph nodes and the right caudal lung lobe. Characteristic tubercles were present in the lung and/or tracheobronchial lymph node of 10 of the 12 animals.

Mycobacterium tuberculosis (Mtb) was cultured from the tracheobronchial lymph node by the National Veterinary Services Laboratory (USDA, APHIS) in this case. Mtb was isolated from lung and/or tracheobronchial lymph node in 7 of 12 animals involved in the outbreak. Genotyping was performed and all isolates shared the same spoligotype and VNTR-11 profile, confirming a common source of infection. The results of tuberculosis testing on this animal from the time of acquisition to death appear in Table 2.

Mtb is an aerobic, nonmotile, nonsporulating, straight to slightly curved 1-4 micron rod-shaped bacillus from the order *Actinomycetales*. Mtb is a member of the *M. tuberculosis* complex, which includes other *Mycobacterium* species that induce tubercle formation including *M. bovis* and its variants *M. caprae* and *M. pinnipedi*, and less frequently identified species *M. africanum*, *M. canetti,* and *M. microti*.[10] The bacterium features a thick, waxy cell wall containing mycolic acids which impart unique characteristics including acid-fast staining positivity and, along with other cell wall components, resistance to environmental desiccation, antibiotics, and phagocyte destruction.

In macaques, infection occurs following inhalation of aerosolized bacteria into the lungs.[7] Ingestion is an infrequently encountered route of inoculation. Resident tissue macrophages phagocytize bacteria,

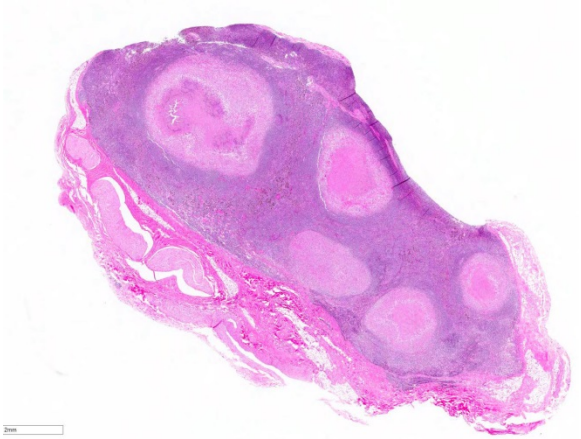

Tracheobronchial lymph node, rhesus macaque. Low magnification of a cross section of the lymph node demonstrates the granulomas seen in Figure 3-1. (HE, 5X)

and through multiple mechanisms, bacteria prevent lysosomal degradation and subsequently replicate within an intracytoplasmic phagosome.[10] Dendritic macrophages may then disseminate bacilli to draining lymph nodes and distant organs. Complex biochemical signaling and immune cell activation pathways, especially of CD4+ and CD8+ T cells, are required for control of primary infection.[2,4,7,9,10] The latent, non-infectious stage ensues when bacteria have been sequestered within granulomas characterized by a central accumulation of necrotic debris that is rarely mineralized surrounded by infected epithelioid macrophages and Langhans multinucleated giant cells, lymphocytes, and a fibrous capsule.[10] Bacteria persist within the tubercle and may reactivate, typically in association with immunosuppression.[5,9] Typical tubercles can be found in any organ and most commonly disseminate from the lungs and hilar lymph nodes to the liver, spleen, kidney, vertebra, and gastrointestinal tract.

Cases of spontaneous and experimental tuberculosis are reported in several primate species with variation in susceptibility to disease.[1,2,4,7,9] Macaques are known to be highly susceptible and present with a disease course of fulminate primary, active-chronic, or latent infection with or without reactivation. Active infection and bacterial shedding can occur over weeks to months, during which time clinical signs may be vague, weight loss and cough, or inapparent.[1,6,9] Intermittent bacterial shedding in latently infected macaques has been documented experimentally, evidenced by sporadic positive bacterial culture of gastric and bronchial alveolar lavage fluids.[9] This finding suggests that disease occurs on a continuum between active and latent infection. Cynomolgus macaques are thought to be relatively more resistant to clinical disease than rhesus macaques, and in experimental studies, 40-50% developed latency.[2,6,9] Spontaneous reactivation of latent infection in the absence of experimental immunosuppression is infrequent, reportedly less than 5% in cynomolgus macaques.[5]

Mtb is an important zoonotic pathogen with potentially devastating effects in captive macaque populations and routine measures have been adopted by US facilities for screening of imported and domestically-reared animals. The most commonly utilized screening test is the tuberculin skin test (TST).[8] MOT, a combination of *Mycobacterium* antigens from multiple species, is injected intradermally, typically into the upper eyelid.[8] The site is checked for reaction at 24, 48, and 72 hours post-injection (see Table 1 for grading).[8] In affected animals, a delayed-type hypersensitivity reaction to antigen produces swelling, erythema, and/or necrosis at the injection site. False negatives may occur in animals with anergy and disseminated disease, and in animals that are in the latent stage of infection.[8] The MOT antigen is not specific for *M. tuberculosis* and *M. bovis*, and false positives may occur in the face of

infection with a non-tubercular *Mycobacterium* species. The TST is the only approved screening test for internationally acquired animals undergoing US quarantine, and three negative tests two weeks apart are the standard requirement.[8] Typically, animals that have cleared international quarantine and domestically reared animals are tested on a semiannual basis.

Alternative commercial tests utilized during this outbreak included the whole-blood interferon gamma (INFγ) test PRIMAGAM® (Prionics USA Inc., La Vista, NE) and the lateral flow immunoassay PrimaTB STAT-PAK® (CHEMBIO).[8] In the PRIMAGAM® test, the concentration of INFγ is measured following incubation with purified protein derivative (PPD) of *M. bovis* (bPPD) and *M. avium* (aPPD).[8] Positive tests that yield a higher reaction to bPPD vs. aPPD indicate sensitization to antigens from either *M. tuberculosis* or *M. bovis*, while a higher aPPD suggests sensitization to *M. avium* and retesting after a 2-week period is recommended.[7] The PrimaTB STAT-PAK® test detects antibody response to three TB-specific antigens (ESTAT-6, CFP-10, MPB83).[8] Serum, whole blood, or plasma can be used.

During this outbreak, the first animal was initially detected by routine tuberculosis surveillance with a positive TST. Affected animals exhibited variable responses to TST, PRIMAGAM®, and PrimaTB STAT-PAK® testing performed during the outbreak. Five months prior to the outbreak this animal exhibited a grade 3 reaction with a TST. A follow-up TST on the contralateral eyelid and PRIMAGAM® and PrimaTB STAT-PAK® tests were all negative. Likewise, all three tests performed at the time of the outbreak were negative. The gold-standard for diagnosis of *M. tuberculosis* is culture,

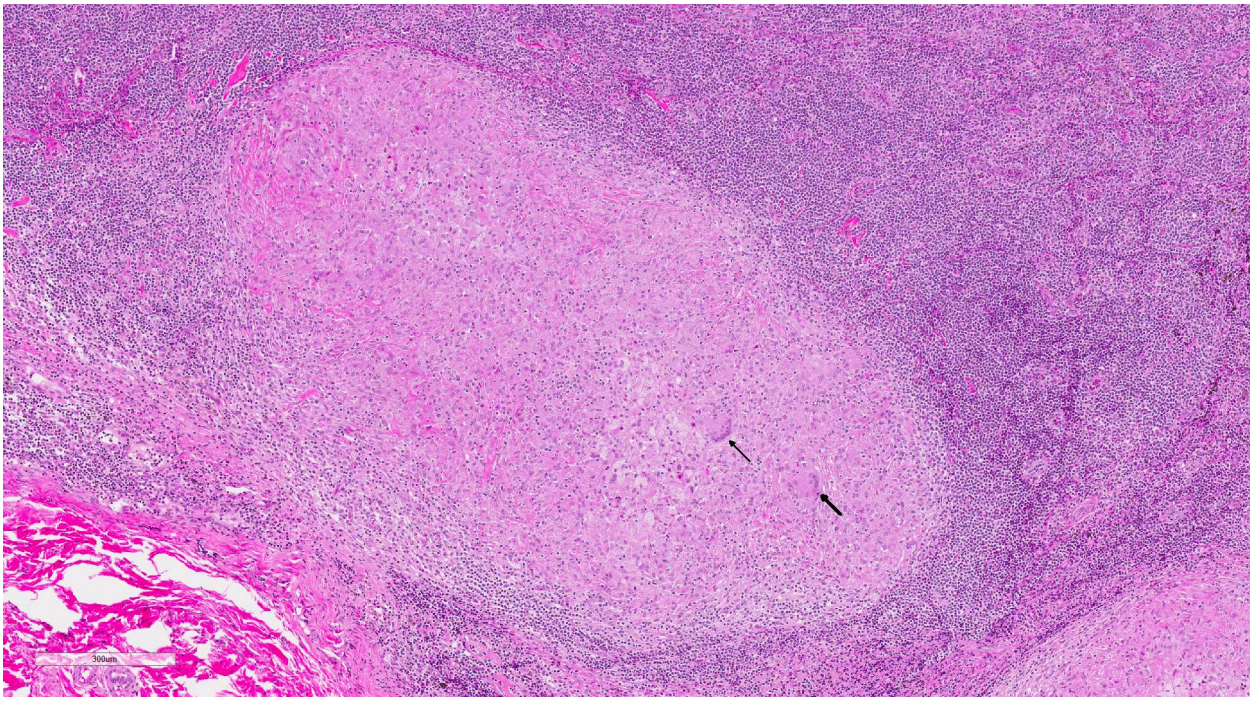

Tracheobronchial lymph node, rhesus macaque. Higher magnification of one of the granulomas. At 75X, several Langhans' giant cells are visible. (HE, 75X)

which was positive for this animal. This outbreak is thought to have occurred as a result of reactivation and shedding from a latently infected animal in the room. The source was not identified. This outbreak illustrates the challenges of antemortem diagnosis and underscores the importance of routine tuberculosis screening as clinical signs were not observed in any of the animals in this cohort.

JPC Diagnosis: Lymph node: Lymphadenitis, granulomatous, multifocal to coalescing, moderate, rhesus macaque, *Macaca mulatta*.

Conference Comment: The contributor provides a fantastic example of one of the classic manifestations of *Mycobacterium tuberculosis* (*Mtb*) in a nonhuman primate. Participants readily identified multifocal to coalescing well organized to nodular tuberculoid granulomas partially effacing the lymph node architecture. The classic tubercle forming bacilli are *Mtb*, primarily infecting humans and nonhuman primates, and *Mycobacterium bovis* affecting bovine species.[3]

Infection is typically via inhalation of aerosol droplets from an infected individual with pulmonary disease. Humans are the only known natural reservoir for *Mtb*. The bacilli then travel to the alveoli where they are phagocytized by alveolar macrophages. The ability of the organism to survive within macrophages is the key to its pathogenicity.[10] Once inside the macrophage, bacilli can survive and replicate by inhibiting the fusion of the phagolysosome, thus preventing oxygen radical formation and avoiding proteolytic enzymes produced by the host macrophage. Natural resistance-associated macrophage protein (NRAMP) is a membrane protein that is involved in innate immunity to

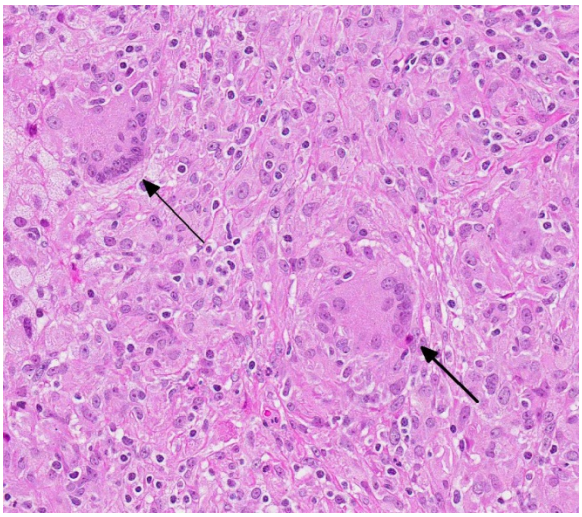

Tracheobronchial lymph node, rhesus macaque. Higher magnification of the Langhans' giant cells. Other multinucleated macrophages are present within this field. (HE, 316X)

infection by *M. bovis* in humans and mice.[1,3,10]

Once exposed to the bacteria, alveolar macrophages are stimulated by ligation of Toll-like receptor 2 (TLR2) and TLR4 to secrete pro-inflammatory cytokines such as tumor necrosis factor-alpha (TNF-alpha), interleukin-1 (IL-1) IL-6 and IL-12, in addition to a variety of C-C chemokines to recruit leukocytes to the site of infection. Alveolar macrophages also present phagocytized mycobacterial antigen to naïve T cells via major histocompatibility complex class II (MHC II).[3,10] This binding to the T-cell receptor and exposure to IL-12 secretion stimulates T cell differentiation to CD4+ T helper 1 (Th1) lymphocytes. These Th1 lymphocytes then secrete interferon gamma (IFN-gamma) and IL-2 stimulating the classical activation of macrophages, favoring a cell mediated immune response. TNF-alpha and IFN-gamma work synergistically to form tuberculoid granulomas in an effort to prevent the spread of the infection to other sites in the body and transmission of the infection to other animals.[3,10] This granuloma is maintained by

a type IV (delayed-type) hypersensitivity (DTH) reaction to persistent antigenic stimulation due to *Mtb*'s ability to survive within macrophages and extracellularly within the granuloma. Ongoing infection eventually leads to caseous necrosis within central area of the granulomas. Interestingly, bacilli can survive for years within the caseous centers and be reactivated by immunosuppression, malnutrition, or concurrent infection.[1,3,10]

Additionally, dendritic cells in the lung also phagocytize *Mtb* by binding receptor DC-SIGN via the bacterial cell wall virulence factors lipoarabinomannan mannose-capped (ManLAM), complement receptor 2 (CR3), and mannose receptor (MR) and then migrate to regional lymph nodes to present mycobacterial antigens to lymphocytes. Spread from the lungs to the tracheobronchial may lymph node may explain the location of the lesion within the tracheobronchial lymph node, in this case.[3,10]

Contributing Institution:

Pathology Services Unit
Department of Animal Resources
Oregon National Primate Research Center
Beaverton, OR 97006
http://onprc.ohsu.edu

References:

1. Bailey C, Mansfield K. Emerging and reemerging infectious diseases of nonhuman primates in the laboratory setting. *Vet Pathol*. 2010; 47(3):462-481.
2. Capuano III SV, Croix DA, Pawar S, et al. Experimental *Mycobacterium tuberculosis* infection of cynomolgus macaques closely resembles the various manifestations of human *M. tuberculosis* infection. *Infect Immunol*. 2003; 71(10):5831-5844.
3. Caswell JL, Willims KJ. Respiratory system. In: Maxie MG ed. *Jubb, Kennedy, and Palmer's pathology of domestic animals.* Vol 2. 6th ed. St. Louis, Missouri: Elsevier; 2016:547-551.
4. Chen CY, Huang D, Wang RC, et al. A critical role for CD8 T cells in a nonhuman primate model of tuberculosis. *PLoS Path*. 2009; Apr; 5(4):1-10.
5. Diedrich CR, Mattila JT, Klein E, et al. Reactivation of latent tuberculosis in cynomolgus macaques infected with SIV is associated with early peripheral T cell depletion and not virus load. *PLoS One*. 2010; 5(3):1-12.
6. Garcia MA, Bouley DM, Larson MJ, et al. Outbreak of Mycobacterium bovis in a conditioned colony of rhesus (Macaca mulatta) and cynomolgus (*Macaca fascicularis*) macaques. *Comp Med*. 2004; 54(5):578-584.
7. King Jr, NW. Tuberculosis. In Jones TC, Mohr U, Hunt RD, eds. *Nonhuman primates 1*. 1st ed. Germany: Springer-Verlage Berlin Heidelberg; 1993:141-148.
8. Lerche NW, Yee JL, Capuano SV, Flynn JL. New approaches to tuberculosis surveillance in nonhuman primates. *ILAR*. 2008; 49(2):170-178.
9. Lin PL, Rodgers M, Le'kneita S, et al. Quantitative comparison of active and latent tuberculosis in the cynomolgus macaque model. *Infect Immunol*. 2009 Oct; 77(10):4631-4642.
10. Sakamoto K. The pathology of *Mycobacterium tuberculosis* infection. *Vet Pathol*. 2012; 49(3):423-439.

CASE IV: 46519 (JPC 4089353).

Signalment: Two-year-old male Fisher 344 rat (*Rattus rattus*).

History: This male rat had been on test for 634 days as part of a 2-year carcinogenesis study; was found dead and reported as a natural death animal.

Gross Pathology: On gross examination, the abdomen was markedly distended with copious amounts of reddish-brown fluid (ascites). In addition, numerous, pale tan, firm, raised nodules were diffusely lining peritoneal viscera; the testes and epididymis were swollen and discolored containing multiple, discrete, pale tan nodules.

Laboratory results: N/A

Histopathologic Description: Testis and epididymis: An unencapsulated, exophytic neoplasm composed of arborizing papillary projections is diffusely infiltrating the vaginal tunic and lining the serosal surfaces of the testis and epididymis, often extending into the adjacent adipose tissue. The neoplasm is comprised of cuboidal epithelial cells, piling up to 4 cell-layers thick and supported by thick, fibrovascular stroma. Neoplastic cells have indistinct cell borders, with small amounts of finely granular, eosinophilic cytoplasm and a single, central, round to oval nucleus with 1-3 variably distinct nucleoli and finely stippled chromatin. Mitotic figures are rare. Anisocytosis and anisokaryosis are mild. Moderate numbers of mast cells with fewer hemosiderin-laden macrophages are scattered throughout the neoplasm. Small caliber vessels occasionally contain aggregates of neoplastic cells admixed with variable amounts of eosinophilic flocculent material (fibrin) and necrotic debris (vascular invasion). Multifocally within the adjacent adipose tissue, vascular lumina are partially occluded by adherent casts composed of fibrin and a mixture of inflammatory cells (vascular thrombosis). The epididymal ducts are devoid of spermatids (hypospermia) and contain numerous sloughed germ cells within their lumina, admixed with necrotic debris (germ cell exfoliation). Aggregates of basophilic, granular material are occasionally found within ducts or the vacuolated epithelial lining (mineralization and degeneration).

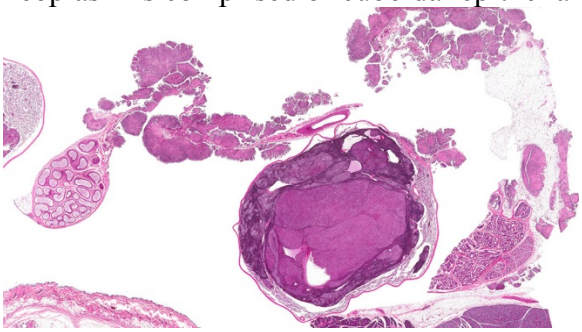

Testis, Fischer 344 rat. The vaginal tunics are expanded by an arborizing proliferative neoplasm (mesothelioma), and the testis is largely effaced by a multinodular neoplasm (interstitial cell tumor) which compresses the remaining seminiferous tubules. (HE, 6X) (Photo courtesy of: EPL, Inc., P.O. Box 12766, Research Triangle Park, NC 27709 http://epl-inc.com/)

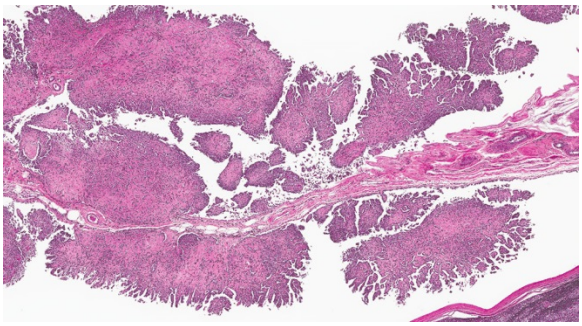

Testis, Fischer 344 rat. The mesothelioma diffusely infiltrates the vaginal tunics and lines the serosal surfaces of the testis and epididymis. (HE, 20X) (Photo courtesy of: EPL, Inc., P.O. Box 12766, Research Triangle Park, NC 27709 http://epl-inc.com

A second approximately 15 x 10mm, discrete, unencapsulated and expansile,

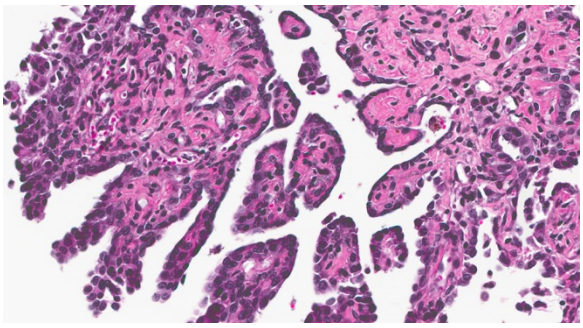

Testis, Fischer 344 rat. The mesothelioma is composed of cuboidal epithelial cells, piling up to 4 cell-layers thick and supported by abundant fibrous stroma. (HE, 400X) (Photo courtesy of: EPL, Inc., P.O. Box 12766, Research Triangle Park, NC 27709 http://epl-inc.com/)

multinodular neoplasm is diffusely effacing and replacing the testicular architecture. The neoplasm is composed of polygonal cells arranged in nests and cords supported by small amounts of fine, fibrovascular stroma. Neoplastic cells have variably distinct cell borders with abundant, finely granular, eosinophilic cytoplasm and a single, round to oval, eccentric to centrally located nucleus containing 1-2 distinct nucleoli and stippled chromatin. Mitotic figures are rare. Anisocytosis and anisokaryosis are mild. Large numbers of lymphocytes are surrounding and infiltrating the neoplasm. The majority of seminiferous tubules are lost; those remaining are shrunken and lined by vacuolated epithelial cells with pyknotic nuclei (tubular degeneration). There are multifocal areas of hemorrhage and mineralization throughout the testis. The contralateral testis is similar in appearance with two, discrete, neoplasms ranging from 2 x 2mm to 3 x 5mm and marked degeneration and atrophy of the seminiferous tubules.

Contributor's Morphologic Diagnoses:

1. Testis, tunica vaginalis: Malignant mesothelioma with vascular invasion and thrombosis.
2. Epididymis: 1) Malignant mesothelioma 2) Diffuse, subacute, severe hypospermia and degeneration with germ cell exfoliation and mineralization.
3. Testis, bilateral: 1) Interstitial cell adenoma, multiple 2) Diffuse, chronic, severe, tubular degeneration and atrophy with unilateral, marked lymphocytic infiltrate and multifocal mineralization.

Contributor's Comment: Spontaneous mesothelioma is a rare neoplasm in rats with an incidence of 0.2–5%, the highest frequencies of which are reported in the Fischer 344 rat strain. Rat mesotheliomas typically occur in aged male rats and originate from the tunica vaginalis with the potential to spread into the peritoneal cavity via transcoelomic extension or seeding.[1-9] To date, 17 studies from the National Toxicology Program have reported xenobiotic-induced mesotheliomas in F344 rats; the F344 rat is particularly sensitive to developing this tumor type and is the only rodent strain reported to develop mesothelioma following xenobiotic exposure by a route other than peritoneal injection.[6,7] Histologically, mesotheliomas may be difficult to distinguish from mesothelial hyperplasia as they can range from a single layer of hyperplastic mesothelial cells lining a thin fibrovascular stroma to papillary projections lined by multiple, irregular layers of cuboidal to polygonal cells that form a pavement or stratified pattern.[1-9] Rat mesotheliomas have a classification scheme similar to humans with sarcomatous, epitheliomatous or mixed types that stain positively with Wilm's tumor 1 (WT-1). Ultrastructural features of mesotheliomas include a distinct basal lamina, junctional complexes between mesothelial cells, microvilli, pinocytotic

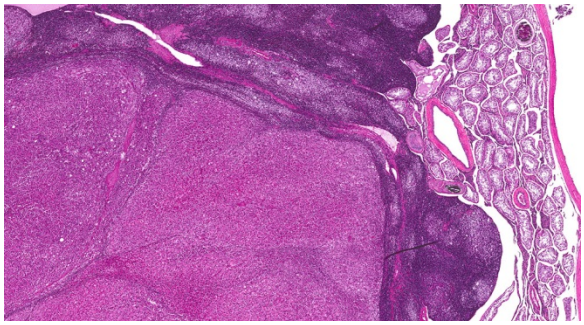

Testis, Fischer 344 rat. A 1.5x1.0cm multilobulated interstitial cell tumor replaces approximately 90% of the testicular parenchyma. (HE, 20X) (Photo courtesy of: EPL, Inc., P.O. Box 12766, Research Triangle Park, NC 27709 http://epl-inc.com/)

vesicles, abundant cytofilaments and dilated rough endoplasmic reticulum (RER).[5-7]

In the male rat, mesotheliomas of the testis, epididymis, and peritoneum are considered to have originated in the tunica vaginalis; all tunica vaginalis mesotheliomas (TVM) are deemed malignant, even those confined to the scrotal sac and lacking features of malignancy, such as local invasiveness, cytological atypia and pleomorphism. Proposed mechanisms of actions for both spontaneous and xenobiotic-induced mesotheliomas include endocrine disruption (leuteinizing hormone, prolactin and testosterone), mechanical stress (compression due to testicular tumors) or oxidative stress (asbestos-induced TVM).[4,6,7]

In the F344 rat, the most common proliferative disorders of the testes include interstitial cell (Leydig cell) hyperplasia and interstitial cell adenoma. Because interstitial cell adenoma is considered a continuum of interstitial cell hyperplasia, it is sometimes difficult to distinguish hyperplasia from adenoma based solely on differences in cellular morphology.[4,7] According to the International Harmonization of Nomenclature and Diagnostic Criteria for Lesions in Rats and Mice (INHAND), Leydig cell hyperplasia typically does not cause compression of the adjacent seminiferous tubules. However, in instances where there is no appreciable compression, proliferative lesions greater than 3 seminiferous tubules in diameter are generally regarded as adenoma.[3,4] Interstitial cell adenomas are common spontaneous and xenobiotic-induced neoplasms of rats and mice, particularly the F344 rat with an underlying pathogenesis that reflects endocrine disruption; a hormonal imbalance between the testicular levels of luteinizing hormone receptor and serum testosterone.

Five mechanisms by which hormone imbalance may contribute to Leydig cell tumor formation have been described and include: estrogen agonists (especially in mice), androgen receptor antagonists, gonadotropin releasing hormone (GnRH) and dopamine receptors, and 5α-reductase inhibitors. Leydig (interstitial) cell adenomas are usually benign, un-encapsulated, discrete neoplasms composed of sheets of uniform polyhedral cells with abundant, finely granular, eosinophilic cytoplasm and a single, centrally located nucleus; compression atrophy of the adjacent seminiferous tubules is common. Leydig cell adenomas are an age-related change, observed most frequently in F344

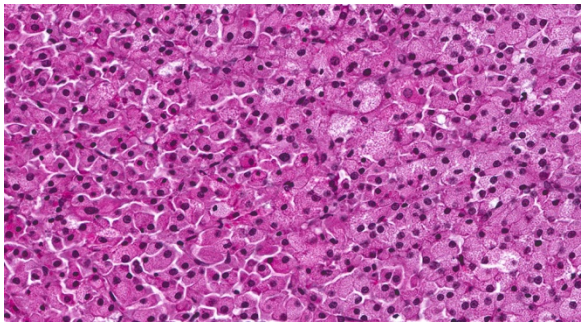

Testis, Fischer 344 rat. Neoplastic Leydig cells have distinct cell borders, vacuolated eosinophilic cytoplasm and mildly anisokaryotic eccentric hyperchromatic nuclei. Mitotic figures are rare. (HE, 200X) (Photo courtesy of: EPL, Inc., P.O. Box 12766 http://epl-inc.com/)

rats in their 2nd year of life, and appear to be inversely correlated with body weight, where increased body weights are associated with higher prolactin levels that reduce Leydig cell tumor incidence.[4,7]

JPC Diagnosis: 1. Testis: Interstitial cell tumor, Fischer 344 rat, *Rattus rattus*.
2. Testis, tunica vaginalis: Mesothelioma.

Conference Comment: The contributor provides an outstanding summary of the pathogenesis of spontaneous and xenobiotic-induced interstitial cell tumor (ICT) and mesothelioma in rats. ICTs (also known as Leydig cell tumor or interstitial adenona) are the most common spontaneous testicular tumor of rats with nearly 100% prevalence in 24-month-old Fisher 344 (F344) rats, as in this case.[8] Additionally, ICTs are commonly multicentric and can occur in one or both testes.[8] Leydig interstitial cells are normally found adjacent to the resident seminiferous tubules in the testis and produce testosterone under the stimulation of luteinizing hormone (LH). Hormonal imbalances as a result of disruption of the hypothalamic-pituitary-testicular axis can result in constitutive LH secretion, which is thought to be the main predisposing feature of ICT formation.[1] ICTs are composed to two cell types readily recognized by conference participants: polygonal cells with granular vacuolated cytoplasm present within the central part of the neoplasm, in this case, and smaller cells with dense hyperchromatic nuclei and scant cytoplasm at the periphery.[8] The conference moderator cautioned participants to not confuse the latter of these two cell types with lymphocytes. Ultrastructurally, interstitial cells contain lipid droplets, abundant smooth endoplasmic reticulum, and numerous mitochondria with tubulovesicular cristae, and desmosomes.[3,8] This neoplasm typically exhibits benign biologic behavior; however, it may be hormonally active and has been associated with hypercalcemia and elevated plasma inhibin levels.[1,3,8] It has a characteristic gross appearance of well-circumscribed yellow hemorrhagic nodules on the testes. Larger masses have areas of mineralization and necrosis.[8]

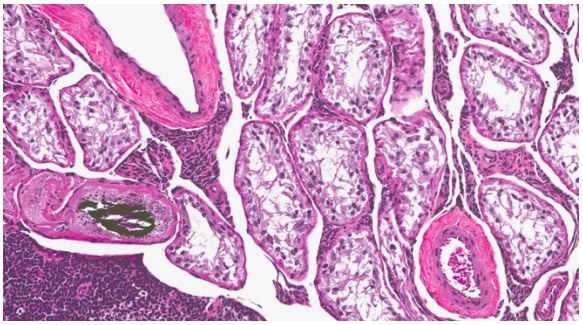

Testis, Fischer 344 rat. Seminiferous tubules at the periphery of the neoplasm are shrunken with a diffuse loss of spermatogonia and lined by a single layer of Sertoli cells in disarray. At bottom left, the periphery of the interstitial cell tumor is composed of numerous small Leydig cells with minimal cytoplasm. (HE, 200X) (Photo courtesy of: EPL, Inc., P.O. Box 12766, Research Triangle Park, NC 27709 http://epl-inc.com/)

Mesotheliomas are the third most common spontaneous testicular tumor of rats and are also particularly common in the F344 strain and they commonly occur concurrently with ICT, as in this case.[8] Mesothelial cells form a lining around the heart, pleural and peritoneal cavities, and the surface of most organs. In males, it extends into the scrotum and tunica vaginalis and wraps the testes and epididymis.[1,2,3,5,8] In male rats, the tunica vaginalis is the most common primary location, with subsequent spread to the rest of the mesothelial-lined surfaces.[8] Interestingly, mesothelalial cells have both an epithelial and mesenchymal component. Stains run by the Joint Pathology Center prior to the conference confirmed immuno-reactivity of neoplastic mesothelial cells to both pancytokeratin and vimentin. Other neoplasms of interest that typically express both vimentin and cytokeratin include: chordoma, synovial sarcoma, meningioma,

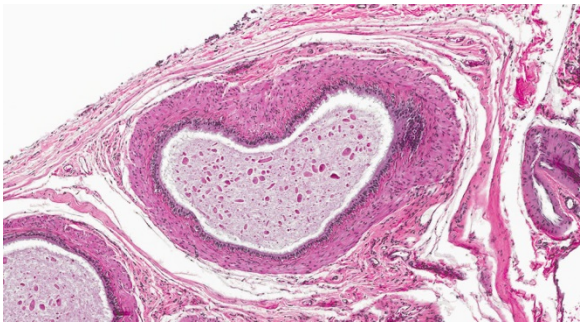

Testis, Fischer 344 rat. Epididymal ducts lack sperm and are filled with numerous sloughed germ cells admixed with cellular debris. (HE, 100X) (Photo courtesy of: EPL, Inc., P.O. Box 12766, Research Triangle Park, NC 27709 http://epl-inc.com/)

renal cell carcinoma, adrenal carcinoma, and endometrial sarcoma.[9] Grossly, mesotheliomas are multiple, well-circumscribed, firm sessile or pedunculated nodules, villous projections, or plaque-like with fibrous adhesions. Concurrent ascites and severe scrotal edema are not uncommon sequelae.[8] Ultrastructurally, mesothelial cells have a microvillous cell membrane, junctional complexes between cells, pinocytotic vesicles, and a distinct basal lamina.[3,5]

As mentioned by the contributor, several studies have attempted to establish a connection between the high incidences of concurrent ICT with mesothelioma in Fisher 344 rats. Some hypotheses include ICT causing direct mechanical stress on mesothelial cells of the tunica vaginalis leading to neoplastic transformation.[1,2] Another theory posits that LH and testosterone secretion by neoplastic ICT cells triggers local mesothelium proliferation. Others suggest that Fisher 344 strain-related sensitivity to chemical exposure causes the development of mesotheliomas and ICTs are an unrelated coincidental background lesion.[1,2] A definitive connection has not yet been established

Contributing Institution:
EPL, Inc.
P.O. Box 12766
Research Triangle Park, NC 27709
http://epl-inc.com/

References:

1. Blackshear PE, Pandiri AR, et al. Gene expression of mesothelioma in vindylidene chloride-exposed F344/N rats reveals immune dysfunction, tissue damage, and inflammatory pathways. *Toxicol Pathol*. 2014; 43:171-185.
2. Blackshear PE, Pandiri AR, et al. Spontaneous mesotheliomas in F344/N rats are characterized by dysregulation of cellular growth and immune function pathways. *Toxicol Pathol*. 2013; 42:863-876.
3. Boorman GA, Chapin BE, Mitsumori K. Testis and epididymis. In: Boorman GA, ed. *Pathology of the Fisher Rat*. San Diego, CA: Academic Press, Inc., 1990: 405-418.
4. Creasy D, Bube A, de Rijk E, Kandori H, Kuwahara M, Masson R, Nolte T, Reams R, Regan K, Rehm S, Rogerson P, Whitney K. Proliferative and nonproliferative lesions of the rat and mouse male reproductive system. *Toxicol Pathol*. 2012; 40: 40S-121S.
5. Hall W. Peritoneum, retroperitoneum, mesentery and abdominal cavity. In: Boorman GA, ed. *Pathology of the Fisher Rat*. San Diego, CA: Academic Press, Inc., 1990: 63-70.
6. Maronpot RR, Zeiger E, McConnell EE, Kolenda-Roberts H, Wall H, Friedman MA. Induction of tunica vaginalis mesotheliomas in rats by

xenobiotics. *Crit Rev Toxicol*. 2009; 39(6):512-537.
7. Maronpot RR, Abraham N, Foreman JE, Ramot Y. The legacy of the F344 rat as a cancer bioassay model (a retrospective summary of three common F344 rat neoplasms). *Crit Rev Toxicol*. 2016; 46(8):641-675.
8. Percy DH and Barthold SW. Rat: Neoplasms. In*:* Percy DH and Barthold SW, eds. *Pathology of Laboratory Rodents and Rabbits.* 4th ed. Ames, IA: Blackwell Publishing, 2016:169-170.
9. Takeshi Y, Tetsuo O, et al. Histochemical and immuno-histochemical characterization of chordoma in ferrets. *J Vet Med Sci.* 2015; 77(4):467-47